J. Fluid Mech. (1994), *vol.* 276, *pp.* 389–403

Bifurcation of rotating liquid drops: results from USML-1 experiments in Space

By T. G. WANG, A. V. ANILKUMAR†, C. P. LEE AND K. C. LIN

Center for Microgravity Research and Applications, Vanderbilt University, Nashville, TN 37235, USA

(Received 29 July 1993 and in revised form 27 April 1994)

Experiments on bifurcation of rotating liquid drops into two-lobed shapes were conducted during a Space shuttle flight. The drops were levitated in air and spinned using acoustic fields in the low-gravity environment. These experiments have successfully resolved the discrepancies existing between the previous experimental results and the theoretical predictions. In the simplest case of a rotating drop that is free from deformation by external forces, the results agree well with the existing theoretical predictions. In the case of a rotating drop subjected to flattening by the acoustic radiation stress, deliberately or otherwise, the experiments suggest the existence of a family of curves, with the free drop as the limiting case.

1. Introduction

The phenomenon of bifurcation of a rotating liquid drop into shapes with two or more lobes, which will be referred to as 'rotational bifurcation' for simplicity, was first observed by Plateau (1863) as a model for a rotating liquid mass held by self-gravity. In his experiment, liquid drops were held and rotated by a shaft in a liquid medium of almost the same density. Beside the solid supporting device, his drops were necessarily influenced by the viscous friction with the outer liquid. We have performed the experiments for liquid drops in air without these limitations, using acoustic force for positioning and acoustic torque for rotation, in the low-gravity environment of the orbiting Space shuttle.

When a spherical liquid drop, held together by surface tension, undergoes a solid-body rotation about say a vertical axis in a less-dense medium, its shape becomes oblate, with its liquid displaced away from the axis owing to centrifugal force in the new equilibrium configuration. With increasing rotation rate, the equilibrium shape becomes more and more flattened, then becomes concave at the top and bottom surfaces, until eventually the two surfaces merge and the central membrane breaks. If the maximum dimension of the drop, which in this case is its equatorial radius, is plotted against the rotation rate, the curve turns upward and then bends back after reaching a maximum rotation rate, before coming to an end corresponding to the meeting of the top and bottom surfaces of the drop (Chandrasekhar 1965; Brown & Scriven 1980). This bending backward of the curve, leading to the multi-valuedness of the maximum dimension with rotation rate there, arises because as the drop extends outward, there is a point beyond which its moment of inertia increases so rapidly that, although its angular momentum keeps increasing, its angular velocity actually decreases.

In reality, however, the drop finds a non-axisymmetric route to equilibrium, which

† Author to whom correspondence should be addressed.

leads to two-lobed ($n = 2$) bifurcation, as the rotation rate reaches a certain critical value before the drop becomes concave (Chandrasekhar 1965). This occurrence can be understood as analogous to the Rayleigh–Taylor instability of an inverted cup of water with the horizontal interface held by surface tension against gravity, the latter playing the role of the centrifugal force in the rotating system. The flat interface becomes neutrally stable and then unstable if its length is increased past a critical value. The axisymmetric shape of the rotating drop also becomes neutrally stable to a two-lobed disturbance as its equator attains a critical dimension at a critical rotation rate. But this is only a crude picture, because the drop surface behaves in a more complicated way than the flat interface, with its two radii of curvature near the equator, both contributing to holding the drop together through surface tension. Although surface tension fails to hold the drop in axisymmetric form against centrifugal force, it can still keep the resulting two lobes of the drop from falling apart (until the drop becomes so elongated that Rayleigh instability of a liquid column takes place at its neck), making it possible for a non-axisymmetric equilibrium shape to exist. More mathematically and elegantly, this effect can be understood in terms of a saddle point on a potential surface (Brown & Scriven 1980). Therefore, unlike the counterpart on the flat interface, the two-lobed shape, beyond the point of neutral stability, is an equilibrium configuration.

The existence of the equilibrium two-lobed shape leads to a side branch bifurcating from the main axisymmetric equilibrium curve. The family of two-lobed shapes branching off from the main axisymmetric family in a plot of the maximum dimension versus rotation rate will be referred to for brevity as the $n = 2$ 'bifurcation curve' from now on. The two-lobed shape is stable if the angular momentum of the disturbed drop is conserved (Brown & Scriven 1980), which is the case in our experiments. The $n = 2$ bifurcation branch of the maximum dimension versus rotation rate curve has been calculated, among others, by Brown & Scriven (1980). With increasing angular momentum, as the drop approaches the other end of the bifurcation branch, at one point the two-lobed shape turns from stable to neutrally stable and then unstable, with the drop eventually fissioning. Brown & Scriven (1980) have also considered another case in which the angular velocity of the disturbed drop is conserved, and obtained the same family of two-lobed shapes branching off from the main axisymmetric family, but found that it is not stable. This case corresponds roughly to Plateau's experiments in which the drops were forced to rotate at certain rates by a solid device. One can find a more detailed historical background to, and other references on, the subject in Brown & Scriven's paper. More recently, Luyten & Callebaut (1983, 1985) studied the stability of uncharged, homogeneously charged, and self-gravitating rotating drops. Luyten (1987) also investigated the stability of a drop corotating with an external fluid of different density. Benner, Basaran & Scriven (1991) studied a two-dimensional analogue of the problem, using a liquid column subjected to planar disturbances.

The means for our experiments, which deal with liquid drops in air (under ordinary atmospheric conditions), is acoustic levitation. It is known that a standing sound field, through its acoustic radiation pressure, can provide a potential well at a pressure node for levitating a small sphere (King 1934). It is also known that two sound fields vibrating in perpendicular directions, at the same frequency but out of phase to generate a circular motion in the medium, can exert a viscous torque on the sphere (Busse & Wang 1981). These are the main principles behind the present apparatus as well as the Drop Dynamics Module (DDM) used in the previous Space experiments (Wang *et al.* 1986). The sound field plays three roles: to support the drop at the middle of the chamber, to deform the drop when needed, and to spin the drop when needed.

In the previous Space experiments, while there was a general qualitative agreement with the theory, there was also some discrepancy between the data and the theoretical curve which needs to be resolved (see §5). Rhim, Chung & Elleman (1988) performed the experiments in a ground-based study using charged drops levitated in an electrostatic field and rotated using an acoustic torque, obtaining an $n = 2$ bifurcation point close to the theoretical prediction. But the use of electric charge and field introduces some uncertainty into the validity of the comparison. Biswas, Leung & Trinh (1991) studied the bifurcation of ground-based acoustically levitated and rotated drops in comparison with the 1986 Space experiments. Although the outcome of their experiments was necessarily biased by gravity, their data have a signature that seems to corroborate that of the earlier Space flight results. We shall come back to this point later.

For the bifurcation study, the results are conveniently displayed in a plot of the dimensionless radius $R^*(R^* = R_{max}/R_0)$ versus the dimensionless rotation rate $\Omega^*(\Omega^* = \Omega/\omega_0)$. Here, R_{max} is the maximum radial position of the axisymmetric or non-axisymmetric drop surface in the equatorial plane from its central axis in gyrostatic equilibrium, R_0 is the spherical radius of the drop, Ω is the drop rotation rate and $\omega_0 = (8\sigma/\rho R_0^3)^{1/2}$ is the $n = 2$ oscillation frequency of the drop, with σ being the surface tension and ρ the density of the drop liquid.

2. Apparatus

The experiments were performed in the Drop Physics Module (DPM) of the United States Microgravity Laboratory-1 (USML-1) onboard the Space shuttle Columbia (STS-50) during its flight starting from June 25 to July 9, 1992, by Astronauts Eugene Trinh and Bonnie Dunbar.

The main part of the apparatus (figure 1) is a 12.7 cm × 12.7 cm × 15.24 cm acoustic chamber made of aluminium walls of thickness 1.27 cm. Four speakers (JBL, custom-made with titanium diaphragm, 30 W) are installed, each at the middle and slightly above each side of the bottom (square) wall, pointing at 45° into the chamber. For the fundamental modes, the horizontal x- and y-axes correspond at 25 °C to approximately 1350 Hz each, and the vertical z-axis corresponds to approximately 1125 Hz. The two speakers facing along x-axis generate the x- and z-waves, and those along the y-axis generate the y- and z-waves, independently. The operating range of the speakers lies between 135 and 155 dB. Three microphones (Endevco), for monitoring the sound pressure levels (SPL) at different frequencies with suitable filtering, are installed: one at the top edge of an x-wall, measuring both the x- and z-wave amplitudes; one at the top edge of a y-wall, measuring both the y- and z-wave amplitudes; and one at a corner of the bottom wall, measuring all of the x-, y- and z-wave amplitudes. Two rectangular quartz windows of thickness 1.27 cm and size 6.35 × 6.35 cm are opened on two opposite sidewalls, and two similar windows of sizes 5.08 × 5.08 cm, and 6.35 × 6.35 cm are opened at the bottom and top walls. Two video cameras (NEC) are installed to photograph the side and top views of the drop, respectively. Also, a 16 mm motion-picture camera (Photosonics) is installed to record both the views, side by side. This is accomplished through an optical image splitting mechanism. The two remaining sidewalls of the chamber have windows to admit light for illuminating the drops. A platinum-resistance temperature sensor (Rosemount) is pasted on one of the sidewalls to monitor the chamber temperature. The video information is available at 60 fields per second, and the motion-picture recording was done at 100 frames per second.

An injector for deploying drops consists of two similar arms sticking out from the

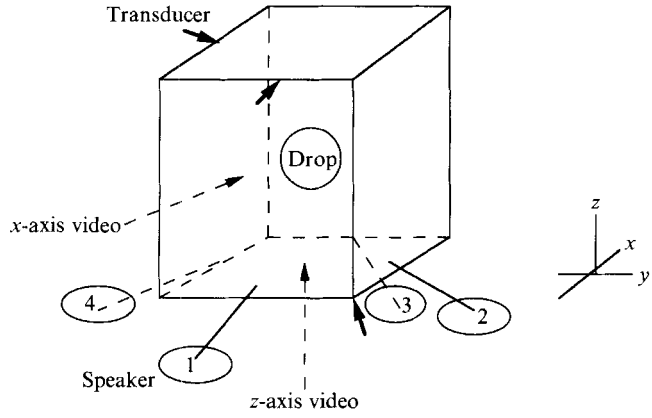

FIGURE 1. Schematic of the Drop Physics Module (DPM).

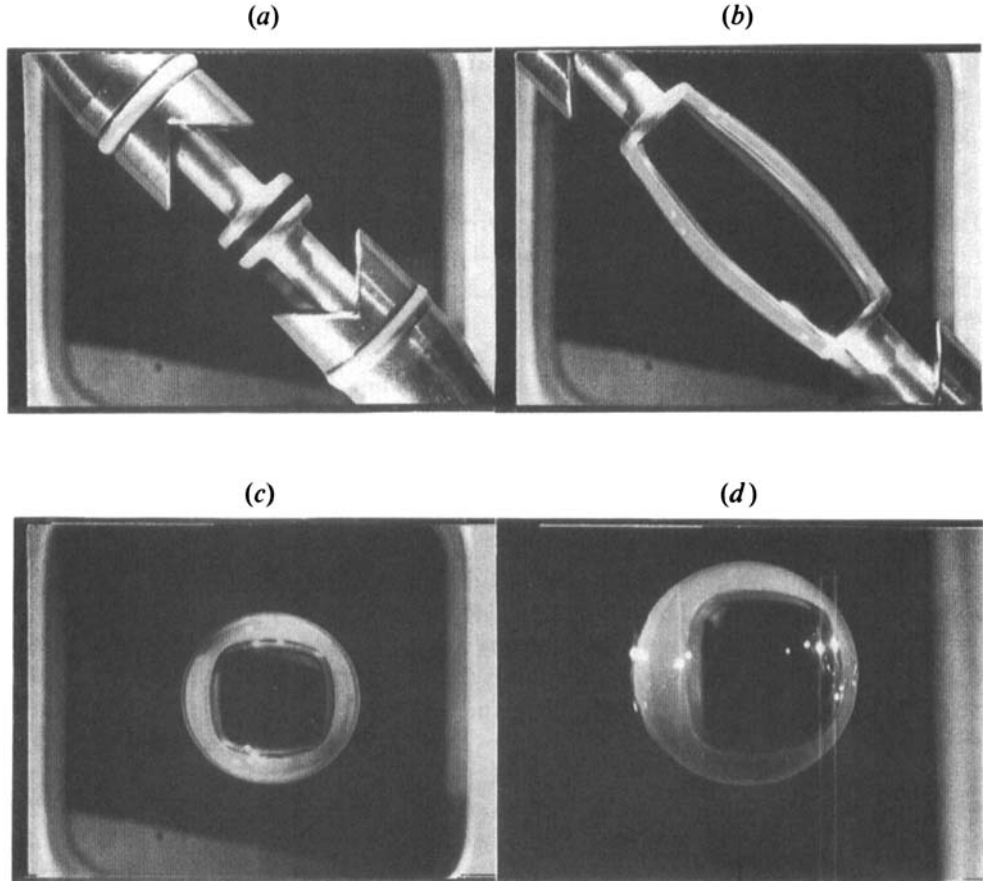

FIGURE 2. Deployment of a silicone oil drop (Session 3): (*a*) top view showing the flat injector tips, (*b*) the injected liquid column, (*c*) the deployed drop, (*d*) side-view of the deployed drop.

middle of two opposite vertical edges to meet at the centre of the chamber when demanded, one of which contains the injector tube for the liquid while the other provides the mechanical means to hold the drop during the injection. Two types of liquids are used for the experiments: (i) silicone oil and (ii) water–glycerine mixtures.

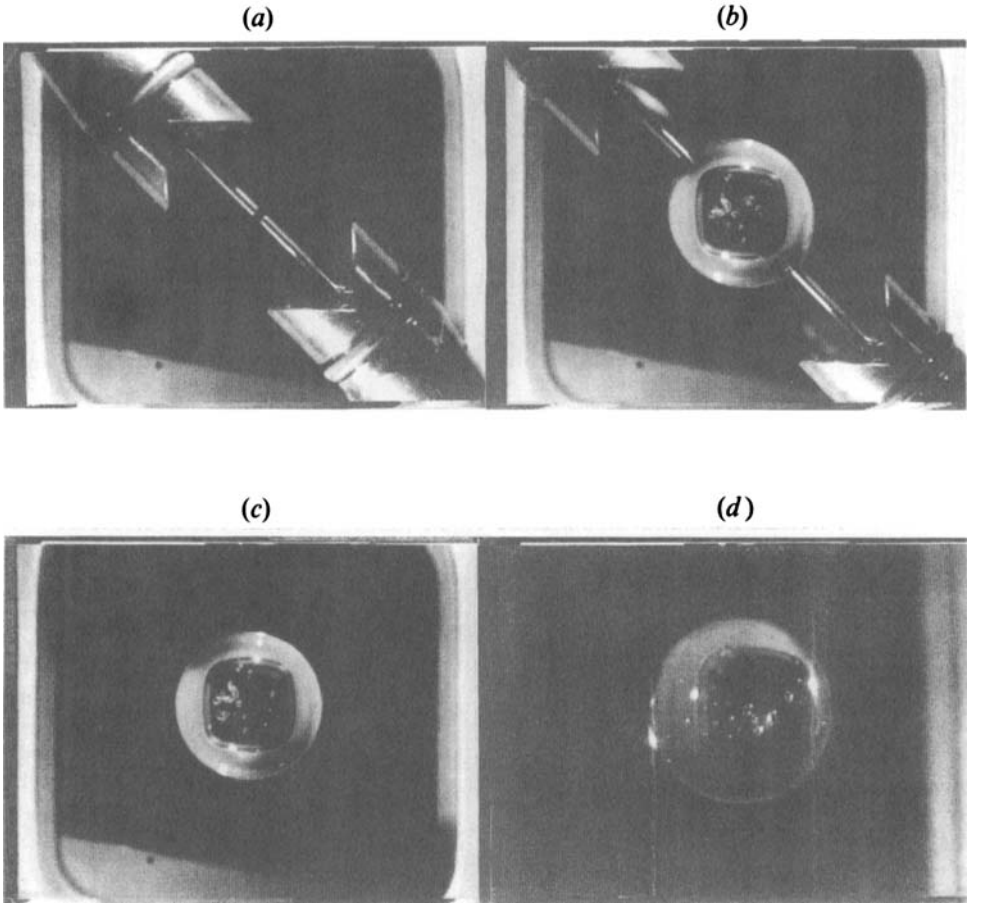

FIGURE 3. Tip–tip deployment of a glycerol–water drop (Session 2): (*a*) top view showing the needle tips, (*b*) the injected liquid drop, (*c*) the deployed drop, (*d*) side-view of the deployed drop.

Since they have different wetting properties they are handled slightly differently. For deploying a silicone oil drop, a flat-tip injector is used such that a liquid column is sandwiched between two flat plates during injection (figure 2). When the desired amount of liquid has been put into place, the arms are suddenly withdrawn, leaving the drop levitated at the centre. The same procedure is used for water–glycerine drops, except that a needle-tip injector is used, such that the drop is held between two needle tips initially (figure 3). A simple tip-to-tip deployment is the desired method, whereby a quiescent spherical drop can be deployed at the centre of the chamber, and easily trapped by the acoustic potential well. This approach, however, was perfected after much practice, and the earlier deployments were collar-to-collar (figure 4). We shall come back to this issue a little later. In general, any satellite drops produced during deployment are trapped in the acoustic potential well like the main drop, and eventually coalesce with the latter.

3. Experimental procedure

The practical absence of gravity allows the study of large drops, and the drop sizes are only limited by how much of a drop can remain in view through the windows while it is deformed by rotation. Since this is mainly a study of the solid-body rotation of

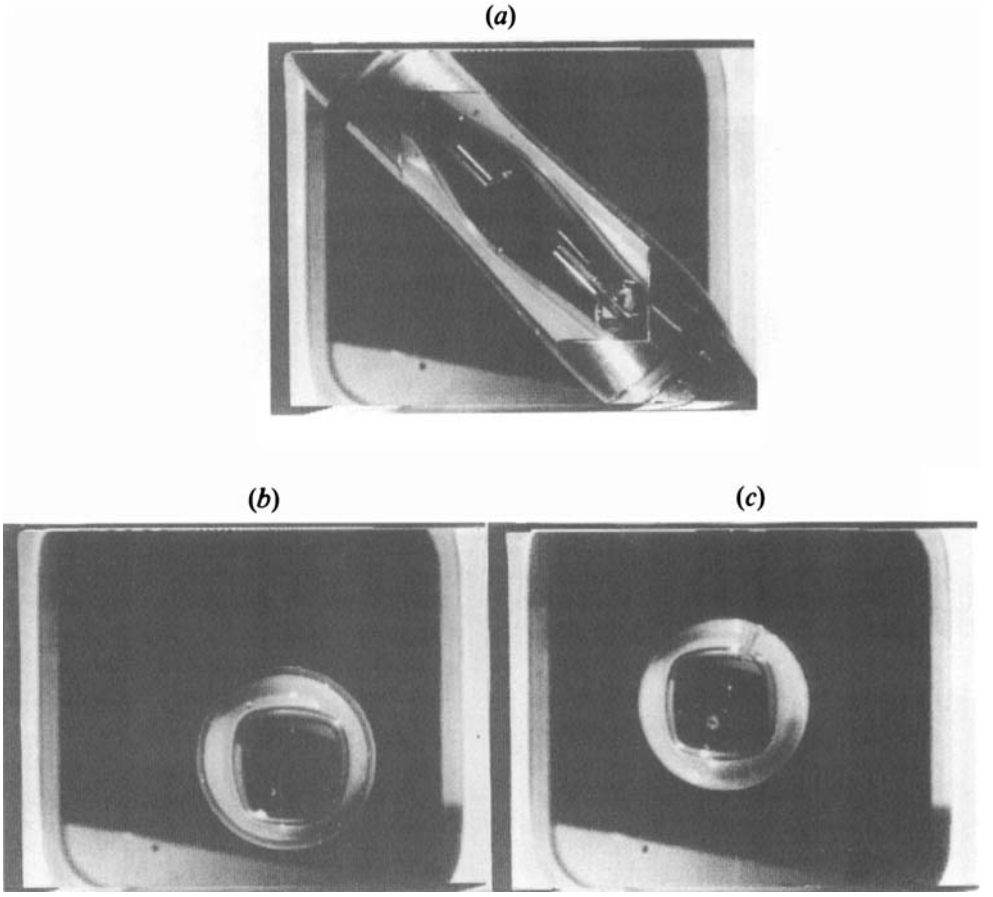

FIGURE 4. Collar–collar deployment of a glycerol–water drop (Session 2): (*a*) top-view showing the liquid column held between collars, (*b*) the launched drop, (*c*) the final stably levitated drop.

Liquid	ν(cSt)	ρ(g cm^{-3})	σ(dyn cm^{-1})
Silicone oil (DC 200 series)	100¶	0.962†	21 ± 0.2*
Glycerine/water (82/18) (with 0.1 % vol. green dye)	47¶	1.209†	64.8 ± 0.4*
Glycerine/water (87/13)	87¶	1.222†	64.4 ± 0.4†

TABLE 1. Properties of the liquids used in the experiments at 25 °C: * measured from leftover flight liquids, † measured from retained samples of the flight liquids, ¶ nominal values suggested by the manufacturer, or from standard tables

drops, transient dynamic situations occurring during spin-up or spin-down have to be minimized. As the relaxation time for a drop to adjust to a new rotation state is inversely proportional to the viscosity of the liquid, only high-viscosity liquids were used.

Silicone oil is the best choice since unlike water, for example, its surface tension is not very sensitive to contamination. This fact is important, considering that because of the flight planning, the liquids had to be prepared and stored for months before the flight. Pure water was not used also because of its low viscosity, which leads to long relaxation times. Glycerine/water (82/18 and 87/13, by weight) solutions were used

instead. The properties of the liquids used are listed in table 1. Tracer particles were used to follow the rotation of the drops, such that a solid-body rotation could be visually recognized when it occurred, and the resulting rotation rate could be measured. Pliolite tracer particles (Goodyear Chemical Co.), about 50–100 μm in size, were mixed with the liquids during preparation.

Although the deployment volume of a drop is predetermined, a small amount of liquid is inevitably lost due to wetting on the injector surfaces. The volume of a drop can be read accurately after it is released and takes on a spherical form. With a viscous drop, surface disturbances typically subside very quickly and if the deployment is neat (figure 3), the volume can be read immediately afterward. However, if the deployment leads to translational oscillations of the drop in the potential well, arising from uneven snapping from the injector collars (figure 4), the volume can be read accurately only after the drop settles down in the potential well, with a reasonably spherical shape. The volume of the drop is calibrated against a perfectly machined 2.54 cm plastic ball when the latter is held at the centre of the chamber by the injector arms.

For the bifurcation study, a drop is levitated and rotated about the z-axis using about 145 dB of sound pressure level along each axes. Minimum acoustic pressures are used to avoid deforming the drop. For spinning a drop, the direction of change of the acoustic torque is known, but the actual magnitude of the torque increment is not known. In the controlled spin-up and spin-down experiments, the torque was changed stepwise (the data points in figures represent the steps), allowing at least 30 s between steps for the drop to relax in order to ensure solid-body rotation. In reality, owing to the high viscosity of the drops, the transient effects decayed very rapidly, in about a second.

In general, during the experiments the drops stays at a fixed position and rotates steadily in gyrostatic equilibrium after its rotation rate has increased past a certain point; thereafter usable data can be taken. Most measurements of the maximum equatorial radius R_{max} were made using the top view (z-view), where the measurements were insensitive to any small movements of the drop.

4. Results

4.1. *General observation*

In general, according to Brown & Scriven (1980), if we plot R^* versus Ω^* for a drop being spinned up from rest slowly enough to guarantee gyrostatic equilibrium at all time, we can obtain a curve on which R^* increases from 1 as Ω^* increases from zero, since the drop becomes increasingly flattened axisymmetrically with rotation. Then at $\Omega^* = 0.56$, where the curve bifurcates, the drop always loses its axisymmetry and becomes two-lobed in shape in practice, moving into the bifurcation branch rather than staying on the main axisymmetric equilibrium curve. On the (Ω^*, R^*)-plane, the bifurcation curve bends backward as the drop extends its two-lobed shape and its angular velocity decreases, while its angular momentum keeps increasing, until the drop fissions.

The bifurcation path can be retraced back and forth with the same drop by slowly increasing or decreasing the acoustic torque. The drop can be held in a steady rotating two-lobed shape at any point on the path indefinitely, by keeping the torque constant to compensate for air friction. On the other hand, if we push the drop to the end of the bifurcation path, the two-lobed shape snaps at the middle, leading to two drops flying apart. The drop can also be led back to the main axisymmetric branch through the bifurcation point if the torque is reduced to a value below the bifurcation point.

4.2. *Error analysis*

The data are sampled after the drop attains gyrostatic equilibrium and stays at a fixed position. Owing to the high spatial and temporal resolution of the drop imaging, the measurement error in drop rotation rate Ω and the maximum equatorial radius R_{max} is extremely low; approximately 0.5% or less. These errors are about the size of the plot symbols used in figures 5–9 and have not been separately indicated. However, the uncertainty in drop volume estimation is about 3% and that in surface tension determination is about 1% (table 1). Thereby, the uncertainty in estimation of ω_0, the $n = 2$ oscillation frequency of the drop, is about 2%. This constitutes a systemic error, for it uniformly shifts the bifurcation curve to the right or to the left. The overall uncertainty in Ω^* is about 2.5% and that in R^* is about 1.5%.

The experiments were conducted in the temperature range 22.5–26.5 °C. The experimental chamber would warm up very slowly (about 1 °C every 25 minutes at the fastest rate) as the experiments progressed. This was mainly due to the continuous operation of the lights and the speakers. But during the timescales of each run, representing a traverse in one direction through the bifurcation curve, the temperature was fairly steady (less than 0.5 °C variation). While plotting the bifurcation curves, the ω_0 for each run has been estimated at the corresponding temperature by correcting the surface tension measurements made at 25 °C (table 1) by -0.16 dyn cm^{-1} °C^{-1} for water–glycerol drops and -0.08 dyn cm^{-1} °C^{-1} for silicone oil drops. It should however be appreciated that even a large temperature fluctuation of 2 °C contributes an error of about 0.4% or less to the data.

The experiments were conducted over three sessions.

4.3. *Practising session*

The first session, with glycerine/water (87/13) solution, was used to understand the operation of the DPM system, namely, the methodology of drop deployment and rotation, and the optimal procedure for conduct of the bifurcation experiments.

The drop was first deployed using a collar-to-collar deployment, as opposed a tip-to-tip one. It was noticed in this learning session that the former method has many disadvantages. It can lead to drop contamination if the collars have been wetted in the deployment of a previous drop of a different liquid (especially so when a surfactant is involved). Furthermore, the strong disturbances resulting from the deployment makes levitation difficult, especially since the drop is launched away from centre of the potential well. Since, as mentioned earlier, the volume of the drop is best evaluated immediately after deployment, the disturbances also make the volume evaluation difficult.

Following deployment and switching on of the acoustic positioning fields, it was noticed that the drop would slowly pick up rotation on the y-axis, owing to the presence of a small unbalanced torque. Therefore it was decided to start the drop rotation along the z-axis almost immediately after deployment. Then it was noticed that the drop did not rotate well along the z-axis unless the z-drive level was higher than the x- and y-ones, such that the drop was slightly flattened in the z-direction. The resulting asymmetries along the x- and y-axes lead to Rayleigh torques that prevent rotations along those axes. (A Rayleigh torque is the net torque acting on a non-axisymmetric object at an arbitrary orientation in a sound field, due to the non-axisymmetric distribution of acoustic radiation stress on its surface (Rayleigh 1882).) Henceforth, it was decided to keep the z-drive level slightly higher to flatten the drop minimally prior to rotation. After the drop became gyrostatically stable, the z-drive

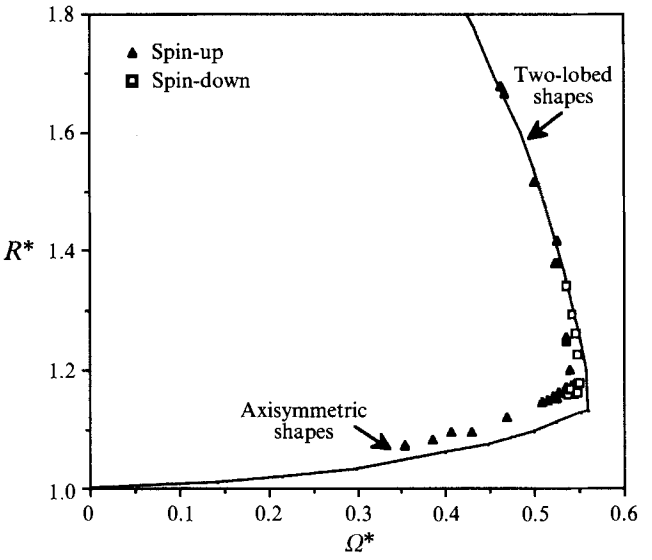

FIGURE 5. Bifurcation diagram showing the evolution of axisymmetric and two-lobed shape families in the dimensionless plot of the maximum equatorial radius versus rotation rate for a 82/18 glycerine/water drop of 2.5 cm^3.

was lowered to match that of the x- and y-axes, as much as possible, to avoid unduly affecting the bifurcation process by the radiation stress. As the experiment progressed, the team learnt to stabilize and rotate the drops with minimal deformations.

4.4. *Data from glycerine/water drops*

In session 2, glycerine/water (82/18) solution, coloured with a green food-colouring dye (McCormick) of 0.1% by volume, was used. The surface-tension measurement (table 1) for this 82/18 solution was made on the ground from the leftover flight sample including the dye.

Figure 4 shows the collar-to-collar deployment of a drop with volume 2.50 ± 0.05 cm^3. Its $n = 2$ oscillation frequency $\omega_0/2\pi$ was experimentally determined to be about 4.0 Hz, compared with the expected value (Lamb 1945, p. 475) of 4.27 Hz from the nominal value of the surface tension (table 1). The difference is very likely due to contamination of the drop liquid by the surfactant left on the collars from an earlier experiment, using surfactant-laden liquids that were deployed collar-to-collar. The temperature during the experiments was 25 °C. In figure 5 we show the data by plotting R^* versus Ω^* for the controlled spin-up and controlled spin-down experiments, with the rotation rate scaled with the experimentally measured value of ω_0. Here 'controlled' implies changing the torque in steps, while adequately pausing between steps to ensure solid-body rotation (the data points represent the steps). The experiment involved a few spin-ups, spin-downs and bifurcations of the same drop, and the data points shown in figure 5 represent about half the runs, where we are satisfied that the drop was in stable levitation and gyrostatic equilibrium; establishing this took several manipulations of the acoustic field. The axisymmetric curve lies slightly above, and the bifurcation branch lies slightly to the left of, the curves predicted by Brown & Scriven (1980).

In figure 6 we show the data for a similar experiment with another drop in session 2, with the drop flattened by the z-drive during spin-up. The drop has a volume of

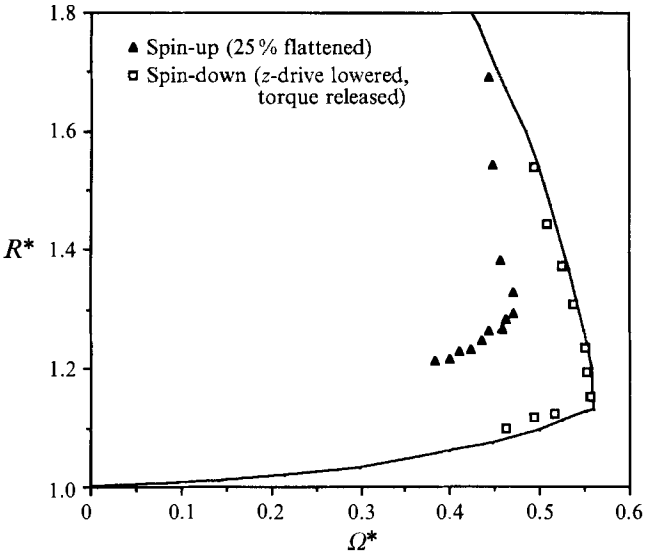

FIGURE 6. Bifurcation diagram for a 82/18 glycerine/water drop of 1.55 cm^3 (the spin-up curve was obtained with the drop deliberately flattened by 25% with the z-drive).

1.55 ± 0.05 cm^3, and was deployed by a tip-to-tip injection between fresh tips (figure 3). The temperature during the experiments was 24 °C. The deformation before the rotation started, defined as $(a/b - 1) \times 100\%$, where a and b are the equatorial and polar radii, respectively, was about $25 \pm 2\%$. For the spin-up, the axisymmetric curve lies well above, and the bifurcation branch lies well to the left of, the predicted ones. The value of Ω^* at bifurcation from the spin-up curve is about 0.47, which is significantly lower than the theoretical value. The bifurcation branch shoots vertically upward such that R^* increases by 10–15% at constant Ω^* before bifurcation. It is noteworthy that bifurcation does not occur at the point where the data curve abruptly changes direction, but a bit above it. Thus the bifurcation point is not well-defined for such a drastically flattened drop. The bifurcation branch continues to rise vertically to intersect the theoretical bifurcation curve. The spin-down was achieved by lowering the z-drive close to (but slightly above) the x- and y-levels, and releasing the torque as opposed to a controlled spin-down. After the drop attained equilibrium following the torque release, it took about 60 s for the drop to spin down from the two-lobed shapes to the axisymmetric shapes. The spin-down curve and the associated bifurcation point agree well with the theory.

4.5. *Data from silicone oil drops*

In session 3, silicone oil (DC 200 series) drops with viscosity of 100 cSt at 25 °C were deployed using special flat tips (figure 2). By this time, sufficient expertise had been acquired in using the apparatus.

The first silicone oil drop had a volume of 2.90 ± 0.05 cm^3. The temperature during the experiment was 22.5 °C. The initial deformation of the drop due to the z-drive was about $6 \pm 1\%$. The torque was carefully raised stepwise for the spin-up. Starting from an axisymmetric shape, the drop went through bifurcation to the two-lobed shape, and then all the way to fission. As seen in figure 7, the agreement with the theory is good, except in the unstable two-lobed region where fission occurs. This issue will be taken up in future work.

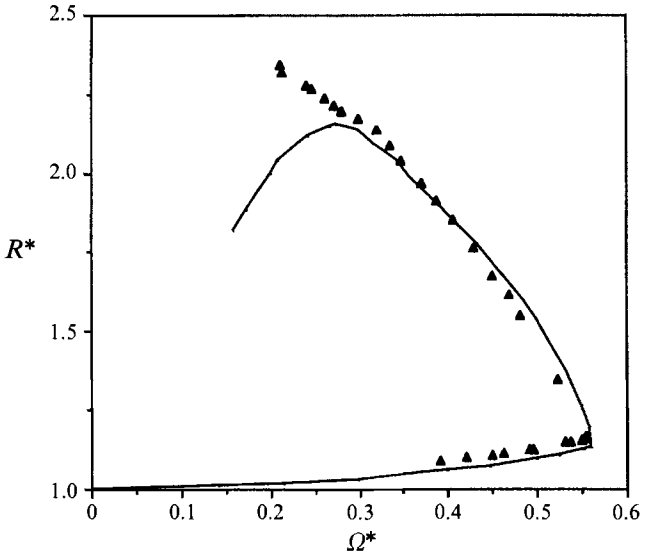

FIGURE 7. Bifurcation diagram for a silicone oil drop of 2.9 cm^3, proceeding all the way to fission (first drop in session 3).

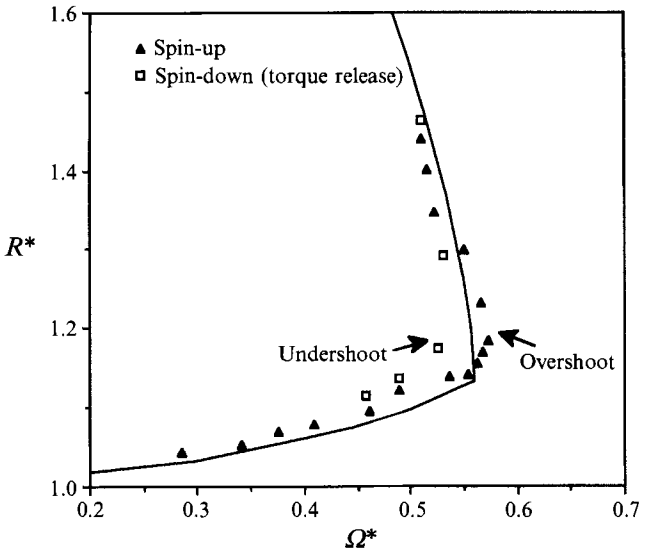

FIGURE 8. Non-equilibrium effects near bifurcation leading to (i) overshooting of the bifurcation point during spin-up, and (ii) undershooting of the bifurcation point during non-ideal torque release (second drop in session 3).

The experiment was repeated with a second silicone oil drop of volume 2.80 ± 0.05 cm^3. It was slightly flattened by the z-drive and first spinned up in discrete steps, initially at a temperature of 24.5 °C. Following bifurcation, there is an overshoot of the bifurcation point (figure 8). In general, during spin-up, following bifurcation there is always an overshooting of the curve as the drop is not in equilibrium just after bifurcation (figure 8). This overshoot depends on the size of the torque increments near bifurcation, and these data are usually not sampled. After the drop attained

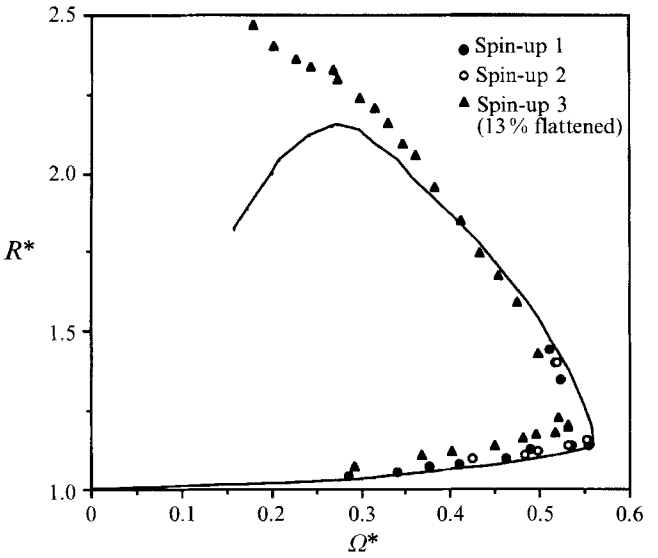

FIGURE 9. Bifurcation diagram for a silicone oil drop of 2.8 cm^3 (second drop in session 3) (the data points leading to fission were obtained with the drop flattened by 13% with the z-drive).

equilibrium, not too high up on the bifurcation curve (see the highest data point along the bifurcation curve in figure 8), the torque was released, with the acoustic positioning still on, to allow the drop to spin down freely due to air friction while being held at the centre of the chamber. In this case, the torque release process was non-ideal (dissipative), manifesting as a disturbance to the drop dimension following release. There is an undershooting of the bifurcation point, leaving the bifurcation curve on the left of the ideal one (figure 8).

In another run at a temperature of 25.5 °C, the drop was spinned step by step beyond bifurcation and then allowed to spin down with all acoustics turned off, starting from a point on the bifurcation curve about the same as that for the previous run. The data for spin-down were lost because, in the absence of any restraining force, the drop moved out of the field of view, and its apparent dimensions changed as it moved toward or away from the camera. But the bifurcation point is estimated to be $\Omega^* = 0.563$, in good agreement with the theory. The difference in the bifurcation point between the spin-down in the previous run and that of this run is noteworthy. Also, the return to axisymmetric shape of the drop was about three times slower in the present case than in the previous case, where the torque release process was dissipative. Finally, the drop was trapped and spinned up past bifurcation to fission, with an initial flattening of 13 ± 1%, and at a temperature of 26.5 °C. As expected, there is a deviation from the theory as a consequence of the flattening (figure 9).

In figure 10(*a–k*), we show photographs of the top view of a typical drop being spinned up from rest, going through bifurcation to fission. Figure 10(*a–c*) depicts the axisymmetric equilibrium shapes, with figure 10(*c*) just prior to bifurcation. Figure 10(*d*) depicts the equilibrium two-lobed shape just following bifurcation, and figure 10(*e–g*) shows the evolving equilibrium two-lobed shapes. Figure 10(*h–k*) shows the dynamic evolution of the two-lobed drop during the fission process, following loss of equilibrium. In this and other runs, the two lobes of the fissioning drop always look

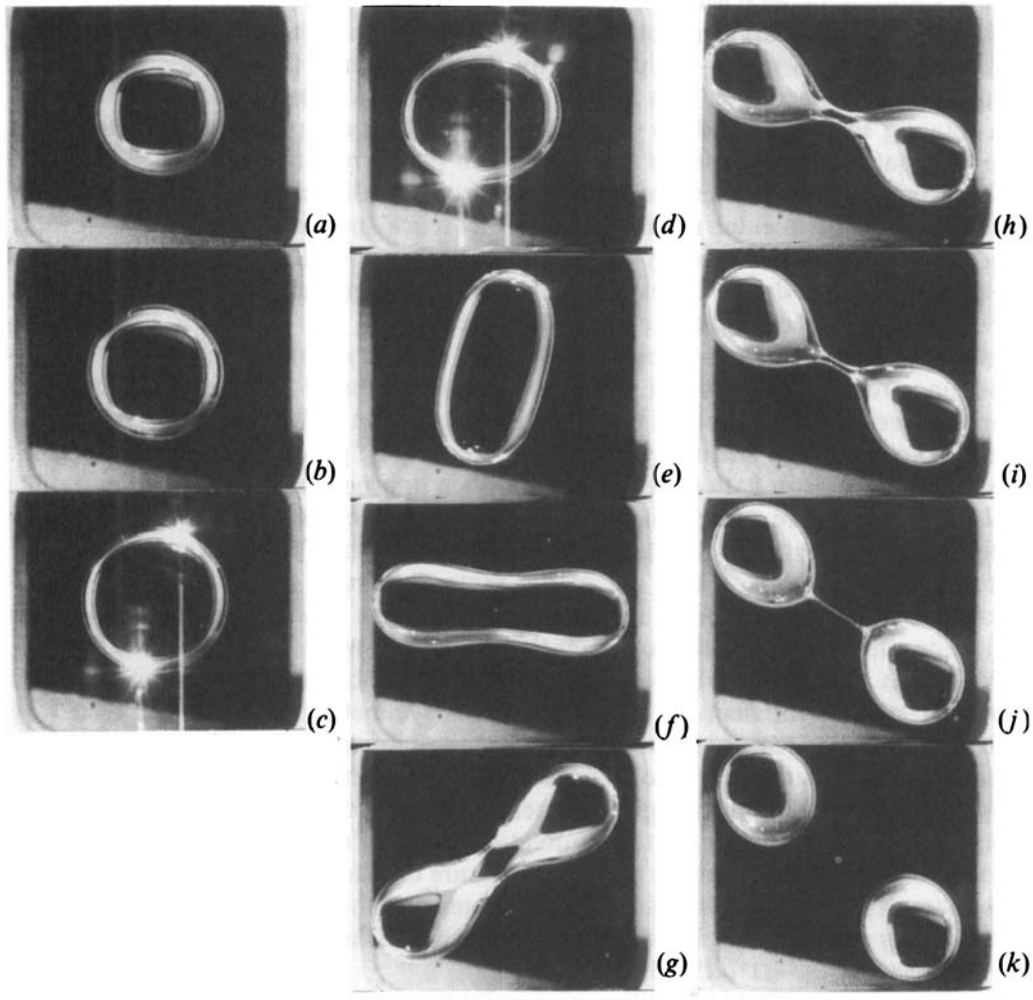

FIGURE 10. Photographs of the top view of a typical drop being spinned up from rest, going through bifurcation to fission: (*a, b, c*) axisymmetric shapes; (*d, e, f, g*) two-lobed shapes; (*h, i, j, k*) necking and fission.

symmetric. During fission (figures 7, 10), it is noted that $R^{*2}\Omega^*$ is approximately constant, as is required by conservation of angular momentum.

It is necessary to flatten the drops to impose a controlled rotation; however, if the imposed deformation is less than about 6% (figure 7), the data agree well with the theoretical predictions of Brown & Scriven (1980).

5. Discussion

In the previous Spacelab experimental results (Wang *et al.* 1986; cf. figure 3), for the spin-up and fission of a 1 cm^3 glycerin–water drop of 100 cSt viscosity, the bifurcation branch lies well to left of the ideal one, crossing the latter at large R^*. The value of Ω^* at bifurcation is about 0.47 ± 0.04, which is below the theoretical value of 0.56. Considering the qualitative similarity between these earlier results and the present

results, shown in figure 6 for the flattened drop, and also those from the ground-based study using a single-axis levitator (Biswas *et al.* 1991), it is felt that the discrepancy in the earlier Spacelab results is due to drop flattening along the rotation axis by the acoustic radiation pressure. This has been confirmed by a re-examination of the initial non-rotating shape of the drop used in the earlier Space experiments, the flattening being estimated to be about the same as that in the current figure 6.

The experiments have been successful in resolving the discrepancies existing between the previous experimental results and the theoretical predictions. In the case of a spherical drop, for which theory exists, the results agree well with the predictions. In the case of flattened drops, the experiments have suggested the existence of a family of curves, with the spherical drop as the limiting case.

In a general context, a rotating drop with its 'elasticity' characterized by the $n = 2$ oscillation frequency is not easily deformed by the acoustic pressure when it is still almost spherical. On the other hand, at the bifurcation point where the stability is neutral, the oscillation frequency is zero and the drop is 'plastic' rather than 'elastic'. Therefore as the drop flattens with rotation when approaching the bifurcation point, it also becomes more susceptible to deformation by the acoustic pressure. In other words, the bias shows up at higher rotation rate. The bias tends to make the drop flatter even if the three waves are of the same amplitude, because after the drop becomes oblate with rotation, it scatters more z-wave than others with its larger projection on the equatorial plane, and thus sees the z-wave as the dominant wave.

With such a bias, it is obvious that the axisymmetric curve should shift upward. Since the angular momentum balance of an axisymmetric drop is not affected by flattening, it seems reasonable to assume that the bifurcation angular momentum is insensitive to the flattening. Also, for the same angular momentum, the axisymmetric drop has a higher R^*, thus a higher moment of inertia and a lower Ω^*. This possibly explains the leftward shift of the bifurcation point. Furthermore, when the drop becomes elongated, the acoustic radiation pressure continues to flatten it such that R^* rises more rapidly with decreasing rotation rate than the non-flattened counterpart. This possibly explains why the bifurcation curve for the flattened drop rises to intersect the ideal one on the (Ω^*, R^*)-plane.

Another question is why the bifurcation point from the ground-based study (Biswas *et al.* 1991) of about $\Omega^* = 0.44$ for an initial deformation of 21% due to the levitating sound field, is lower than the 0.47 for a drop of an even greater deformation of 25% in figure 6, if we believe that the bifurcation point should decrease with deformation. A reasonable explanation is that although gravity is much weaker than surface tension in the ground-based study, it can easily tip the energy balance at the bifurcation point, where surface tension is counteracted by centrifugal force to the point that the system is neutrally stable. Gravity tends to spread the drop out horizontally (like a drop on a table), increasing R^* and reducing Ω^* for the same angular momentum.

The data analysis described in this paper was carried out at the Center for Microgravity Research and Applications at Vanderbilt University, under contract with the National Aeronautics and Space Administration. The authors wish to express their gratitude to Dr Eugene Trinh, and Dr Bonnie Dunbar for their tireless efforts in conducting the experiments during the USML-1 mission. The authors are also indebted to Mr Arvid Croonquist, and Dr Mark Lee for their selfless contribution to the success of these experiments.

REFERENCES

BENNER, R. E., BASARAN, O. A. & SCRIVEN, L. E. 1991 Equilibria, stability and bifurcations of rotating columns of fluid subjected to planar disturbances. *Proc. R. Soc. Lond.* A **433**, 81–99.

BISWAS, A., LEUNG, E. W. & TRINH, E. H. 1991 Rotation of ultrasonically levitated glycerol drops. *J. Acoust. Soc. Am.* **90**, 1502–1507.

BROWN, R. A. & SCRIVEN, L. E. 1980 The shape and stability of rotating liquid drops. *Proc. R. Soc. Lond.* A **371**, 331–357.

BUSSE, F. H. & WANG, T. G. 1981 Torque generated by orthogonal acoustic waves – theory. *J. Acoust. Soc. Am.* **69**, 1634–1638.

CHANDRASEKHAR, S. 1965 The stability of a rotating liquid drop. *Proc. R. Soc. Lond.* A **286**, 1–26.

KING, L. V. 1934 On the acoustic radiation pressure on spheres. *Proc. R. Soc. Lond.* A **147**, 212–240.

LAMB, H. 1945 *Hydrodynamics*, 6th edn. Dover.

LUYTEN, P. 1987 Stability of rotating liquid drop immersed in a corotating fluid with different density. *Proc. R. Soc. Lond.* A **414**, 59–82.

LUYTEN, P. & CALLEBAUT, D. K. 1983 Stability of rotating liquid drops: I. Uncharged drops. *Phys. Fluids* **26**, 2359–2367.

LUYTEN, P. & CALLEBAUT, D. K. 1985 Stability of rotating liquid drops: II. Homogeneously charged or self-gravitating drops. *Phys. Fluids* **28**, 2344–2351.

PLATEAU, J. A. F. 1863 Experimental and theoretical researches on the figures of equilibrium of a liquid mass withdrawn from the action of gravity. *Annual Report of the Board of Regents of the Smithsonian Institution, Washington, DC*, pp. 270–285.

RAYLEIGH, LORD 1882 On an instrument capable of measuring the intensity of aerial vibrations. *Phil. Mag.* **14**, 186.

RHIM, W. K., CHUNG, S. K. & ELLEMAN, D. D. 1989 Experiments on rotating charged liquid drops. *AIP Conf. Proc.* 197: *Drops and Bubbles, 3rd Intl Colloqu. Monterey, CA, 1988* (ed. T. G. Wang). AIP.

WANG, T. G., TRINH, E. H., CROONQUIST, A. P. & ELLEMAN, D. D. 1986 Shapes of rotating free drops: Spacelab experimental results. *Phys. Rev. Lett.* **56**, 452–455.